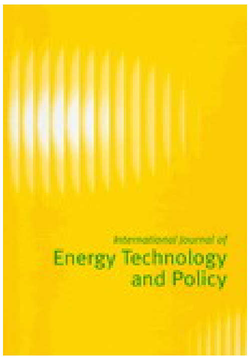

International Journal of Energy Technology and Policy

ISSN online: 1741-508X - ISSN print: 1472-8923
https://www.inderscience.com/ijetp

Method for predicting comprehensive energy demand in industrial parks based on echo state networks

Xiaojun Zhu, Yan Li, Decheng Wang, Qun Zhang, Yinzhe Xie, Na Li, Zhu Chen

DOI: 10.1504/IJETP.2024.10061515

Article History:

Received:	18 May 2023
Last revised:	19 June 2023
Accepted:	19 October 2023
Published online:	10 May 2024

Method for predicting comprehensive energy demand in industrial parks based on echo state networks

Xiaojun Zhu, Yan Li, Decheng Wang and Qun Zhang

State Grid Jiangsu Electric Power Design Consulting Co., Ltd.,
Nanjing, Jiangsu Province, 210008, China
and
State Grid Jiangsu Electric Power Co., Ltd.,
Economic Research Institute,
Nanjing, Jiangsu Province, 210008, China
Email: 398083339@163.com
Email: liyan20211126@163.com
Email: dechengw76@126.com
Email: zq0706031633@sina.com

Yinzhe Xie*, Na Li and Zhu Chen

East China Electric Power Design Institute of
China Power Engineering Consulting Group,
Huangpu District, Shanghai, 200001, China
Email: 2770@ecepdi.com
Email: 2802@ecepdi.com
Email: 2899@ecepdi.com
*Corresponding author

Abstract: To achieve accurate prediction of energy demand, this study designed a new method for predicting comprehensive energy demand in industrial parks using echo state networks. Firstly, analyse the comprehensive energy structure of the park, then collect and supplement historical comprehensive energy load consumption data. Secondly, select the factors that affect the load demand forecast, and calculate the comprehensive similarity of similar days of historical energy demand according to the mutual information between the influencing factors. Finally, input the calculation results into the optimised echo state network of the crossbar algorithm, and output the predicted comprehensive energy demand of the park. Experiment shows that after applying this method, the predicted values fluctuate between 1.410%–2.384%, RMSE values fluctuate between 176.4 MW–205.3 MW, indicating that the error of the predicted results using this method is relatively small.

Keywords: comprehensive energy system of the park; energy demand; cold/hot/electrical loads; crossover algorithm; echo state network; demand forecast.

Reference to this paper should be made as follows: Zhu, X., Li, Y., Wang, D., Zhang, Q., Xie, Y., Li, N. and Chen, Z. (2024) 'Method for predicting comprehensive energy demand in industrial parks based on echo state networks', *Int. J. Energy Technology and Policy*, Vol. 19, Nos. 1/2, pp.2–16.

Biographical notes: Xiaojun Zhu received her Master's in Electrical Engineering from School of Electrical Engineering of Southeast University in 2016. She is engaged in energy storage research, power grid planning in State Grid Jiangsu Electric Power Design Consulting Co., Ltd. and State Grid Jiangsu Electric Power Co., Ltd. Economic Research Institute.

Yan Li received her Master's in Electrical Engineering from School of Electric Power Engineering of South China University of Technology in 2006. She is engaged in integrated energy research in State Grid Jiangsu Electric Power Design Consulting Co., Ltd. and State Grid Jiangsu Electric Power Co., Ltd. Economic Research Institute.

Decheng Wang received his Master's in Power Engineering and Engineering Thermophysics from School of Energy and Environment of Southeast University in 2020. He is engaged in integrated energy research in State Grid Jiangsu Electric Power Design Consulting Co., Ltd. and State Grid Jiangsu Electric Power Co., Ltd. Economic Research Institute.

Qun Zhang received his Master's in Control Engineering from School of Automation of Southeast University in 2017. He is engaged in energy storage research, power grid planning, integrated energy research in State Grid Jiangsu Electric Power Design Consulting Co., Ltd. and State Grid Jiangsu Electric Power Co., Ltd. Economic Research Institute.

Yinzhe Xie received his Master's in Electrical Engineering from School of Electrical Engineering of Zhejiang University in 2013. He is engaged in energy storage research, power grid planning, integrated energy research in East China Electric Power Design Institute of China Power Engineering Consulting Group.

Na Li received her Master's in Electrical Engineering from School of Electrical Engineering of Zhejiang University in 2013. She is engaged in energy storage research, integrated energy in East China Electric Power Design Institute of China Power Engineering Consulting Group.

Zhu Chen received her Master's in Electrical Engineering from Viterbi School of Engineering of University of Southern California in 2014. She is engaged in power grid planning, integrated energy research in East China Electric Power Design Institute of China Power Engineering Consulting Group.

1 Introduction

Industrial parks are an important component of China's industrial clusters and also the allocation centre for production factors in various industries. Nowadays, new energy is widely used globally to improve environmental pollution issues, but there is a phenomenon of structural irrationality in the actual use process. To cope with this situation, the park's energy supply system, mainly based on comprehensive energy has been put into use (Zhao et al., 2022). The comprehensive energy system is an integrated system of multiple energy production, supply, and sales. During the planning, construction, and operation stages, it improves the synergy between energy production, transformation, transmission, consumption, and storage, effectively improving the energy utilisation efficiency and new energy consumption capacity of the park (Zhang et al., 2023; Huang et al., 2022). Due to the large amount of intermittent energy present at the supply end of the integrated energy system, and the presence of multiple types, diverse characteristics, and randomly changing loads at the energy receiving end, it is necessary to analyse the comprehensive energy demand (Luo et al., 2020).

For this purpose, a method for predicting energy demand was designed in Wu et al. (2021a) for the multi energy complementary system in the park. After analysing the environmental factors that affect the demand for cold and hot energy in the park, this method combines the mutual information method with the error minimisation method to preliminarily analyse the demand for energy. On this basis, a method for selecting energy consumption similar days based on comprehensive distance and trend similarity was designed to address the drawbacks of conventional grey correlation analysis. Based on the results of selecting similar energy consumption days, a deep belief network is used to predict the demand for different types of energy loads in the park. In Xu et al. (2020), relevant scholars fully utilised artificial intelligence technology, integrating convolutional neural networks and deep confidence networks, two classic network algorithms, to design a multi type energy demand prediction method. This method first analyses the feature information of convolutional neural networks and extracts effective features from them. Then, the feature extraction results are added as input information to the deep confidence network, and the final energy demand prediction value is output through training and learning. Based on the historical characteristics of energy demand in Fang et al. (2020), the historical feature data is smoothed through linear regression analysis to extract the linear changes of the historical feature data. Then, use the grey linear regression equation to preliminarily predict the trend of energy demand changes in the future stage. On this basis, the weighted fuzzy theory is used to optimise the traditional Markov chain model, modify the preliminary prediction results of the grey linear regression equation, avoid local fluctuations in the energy demand prediction process, and obtain effective prediction results.

However, in practical applications, it has been found that the traditional methods mentioned above still have high prediction errors, and the numerical performance of the MAPE and RMSE indicators is not ideal. In response to this issue, this study proposes a method for predicting the comprehensive energy demand in industrial parks based on echo state networks:

Firstly, analyse the comprehensive energy structure of the park, including the energy supply side, energy hubs, energy storage devices, and load side;

Secondly, collect historical data on the comprehensive energy consumption of the park, and to avoid affecting the reliability of subsequent predictions due to abnormal or missing data, use Lagrange interpolation to repair the data and fill in any missing values;

Once again, based on the observation of historical energy consumption data, it can be seen that the demand for comprehensive energy in the park is actually the demand for cooling/heating/electricity/gas loads. Therefore, the average and upper and lower limit values of temperature, humidity, wind speed and light are selected as the influencing factors of energy demand forecast, and the mutual information value among these four influencing factors is calculated;

Then, according to the analysis results of mutual information of influencing factors, calculate the distance similarity and trend similarity of historical energy demand, and calculate the comprehensive similarity of similar days of historical energy demand through iterative summation;

Finally, the vertical and horizontal crossover algorithm is introduced to optimise key parameters such as echo state network weights and thresholds by initialising the echo state network through horizontal/vertical crossover and comparing competition operators. Input the comprehensive similarity into the echo state network, and after training in the reserve pool, the comprehensive energy demand prediction results of the park can be obtained.

2 Analysis of the comprehensive energy structure of the park

Analysing the comprehensive energy structure of the park can roughly grasp the demand for energy supply, energy hubs, energy storage devices, and load terminals. This is the foundation for planning and construction of the park, and also an important basis for rational layout of the park (Huang et al., 2020).

Firstly, analyse the structure of the comprehensive energy system in the park, as shown in Figure 1.

Figure 1 Comprehensive energy structure diagram of the park

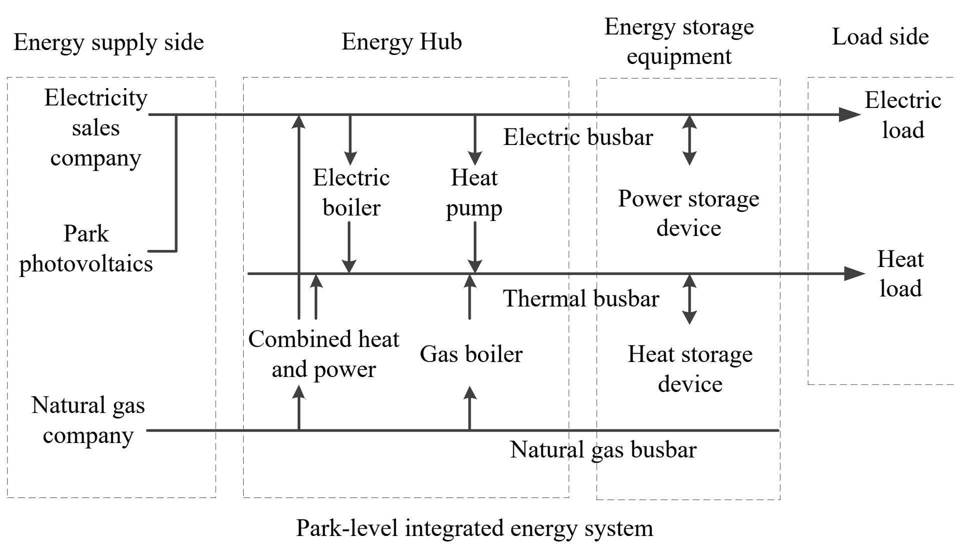

In Figure 1, the comprehensive energy structure of the entire park includes the energy supply end, energy hub, energy storage unit, and energy load end. The energy supply end can provide the initial form of energy, with a portion converted into the required energy form for the energy load end in the energy hub, and the other portion transported to the energy storage unit (Zheng et al., 2022).

A hub is an energy conversion device that can convert different types of energy into the energy required by the energy load end (Zhang et al., 2022). The energy hub has dual ports, where the input energy is $P^{s_i}\,(i = 1, 2, \cdots, p)$ and the output energy is $Q^{s_j}\,(j = 1, 2, \cdots, q)$. Here, p and q represent the types of energy input and output, respectively. The energy conversion process in the hub is as follows:

$$\begin{bmatrix} Q^{s_1} \\ Q^{s_2} \\ \vdots \\ Q^{s_q} \end{bmatrix} = \begin{bmatrix} \delta^{s_1 s_1} \vartheta^{s_1 s_1} & \delta^{s_2 s_1} \vartheta^{s_2 s_1} & \cdots & \delta^{s_p s_1} \vartheta^{s_p s_1} \\ \delta^{s_1 s_2} \vartheta^{s_1 s_2} & \delta^{s_2 s_2} \vartheta^{s_2 s_2} & \cdots & \delta^{s_p s_2} \vartheta^{s_p s_2} \\ \vdots & \vdots & \ddots & \vdots \\ \delta^{s_1 s_q} \vartheta^{s_1 s_q} & \delta^{s_2 s_q} \vartheta^{s_2 s_q} & \cdots & \delta^{s_p s_q} \vartheta^{s_p s_q} \end{bmatrix} \times \begin{bmatrix} P^{s_1} \\ P^{s_2} \\ \vdots \\ P^{s_p} \end{bmatrix} \tag{1}$$

In formula (1), s_i and s_j represent the energy forms of input and output, respectively; $\delta^{s_p s_q}$ represents the efficiency of converting energy s_i into s_j; $\vartheta^{s_p s_q}$ represents the distribution coefficient of energy, which satisfies the following constraints:

$$\begin{cases} 0 \le \vartheta^{s_p s_q} \le 1 \\ \sum_{s_j} \vartheta^{s_p s_q} = 1 \end{cases} \tag{2}$$

3 Analysis of factors influencing energy demand

3.1 Historical energy data preprocessing

Generally speaking, the length of historical data should be long enough to ensure that the prediction model can capture trends and periodic changes in energy demand, but it should not be too long, otherwise it may contain outdated information or noise. Therefore, in this study, the length of historical energy data was set to 8765 data points to avoid adverse effects on prediction performance.

When collecting historical energy consumption data, human error, instrument failure and other problems may occur, resulting in incomplete data or outlier (Xue et al., 2022). To address this issue, this study used Lagrangian interpolation to repair the data and fill in any missing values. The calculation process of the Lagrangian interpolation method is as follows:

$$x_i = \frac{x_{i-1} + x_{i+1}}{2} \tag{3}$$

In formula (3), x_i represents the processed data; x_{i-1} and x_{i+1} represent the previous and subsequent items of abnormal data.

Due to the diverse sources of influencing factors and significant dimensional differences, in order to treat each influencing factor without differentiation, the maximum minimum method was used to normalise each influencing factor. The process is as follows:

$$x_i' = \frac{\overline{x}_i - \overline{x}_{\min,j}}{\overline{x}_{\max,j} - \overline{x}_{\min,j}} \tag{4}$$

In formula (4), x'_i represents the normalised energy consumption data; $\overline{x}_i$ represents the initial energy consumption data; $\overline{x}_{\max,j}$ and $\overline{x}_{\min,j}$ represent the upper and lower limits of the j^{th} influencing factor matrix.

3.2 Calculation of influencing factors mutual information

Based on the analysis of the comprehensive energy system in the previous chapter, it can be seen that the demand for comprehensive energy in the park is actually the demand for cooling/heating/electricity/gas loads. Therefore, this study analyses the influencing factors of cooling, heating, and power loads.

Due to the influence of multiple influencing factors, the cold/hot/electricity/gas load series has significant randomness and volatility. Therefore, the scientific selection of these influencing factors will help improve the accuracy of subsequent predictions (Zheng et al., 2021; Zhu et al., 2022).

This study selects the average and upper and lower limits of temperature, humidity, wind speed, and light as the influencing factors for energy demand prediction, represented as:

$$I = \left[I_1, I_2, \cdots, I_i, \cdots, I_n \right] \tag{5}$$

In formula (5), I_i represents the i^{th} influencing factor matrix; $n = 12$.

Due to the multiple influencing factors involved, the computational complexity of predicting energy demand in the park has greatly increased, especially with some influencing factors having only weak or even inverse correlations with energy supply, which can easily lead to a decrease in estimation accuracy. Therefore, this study selects energy consumption similar days based on the principle of minimum error.

Mutual information can reflect the relationship between different variables (Zhuo et al., 2022). Based on the cooling/heating/electricity/gas load data and its influencing factors, calculate the direct mutual information values of different influencing factors:

$$G\left(I_i, I_v\right) = \sum\nolimits_{I_{it} \in I} \sum\nolimits_{I_{vt} \in I_v} \left(p\left(I_{it}, I_{vt}\right)\right) \log \frac{p\left(I_{it}, I_{vt}\right)}{p\left(I_{it}\right) p\left(I_{vt}\right)} \tag{6}$$

In formula (6), I_{it} represents the value of the i^{th} influencing factor at time t; I_{vt} represents the energy consumption load at time t; $p(I_{it})$ and $p(I_{vt})$ represent the edge distribution of I_{it} and I_{vt}, respectively; $p(I_{it}, I_{vt})$ represents the probability density function.

4 Prediction of comprehensive energy demand in the park

4.1 Comprehensive energy demand similarity analysis

Taking the energy demand influencing factors analysed above as constraints, this study analyses the distance similarity of energy demand and the trend similarity of energy demand, respectively, to calculate the comprehensive similarity of energy demand.

4.1.1 Calculation of distance similarity in energy demand

Assuming that K_i represents the sample influencing factors and K_a represents the corresponding influencing factors for the predicted day, establish the energy demand influencing factor matrix as follows:

$$K = \begin{bmatrix} K_{a1} & K_{11} & \cdots & K_{i1} & \cdots & K_{p1} \\ \vdots & \vdots & \vdots & \vdots & \vdots & \vdots \\ K_{aj} & K_{1j} & \cdots & K_{ij} & \cdots & K_{pj} \\ \vdots & \vdots & \vdots & \vdots & \vdots & \vdots \\ K_{ap} & K_{1q} & \cdots & K_{iq} & \cdots & K_{pq} \end{bmatrix} \tag{7}$$

In formula (7), p represents the number of influencing factors; q represents the dimension; K_{ij} represents the numerical result of the i^{th} influencing factor at time j; K_{aj} represents the numerical value of the influencing factors corresponding to the predicted day at the j^{th} moment (Wang et al., 2022b).

Based on the setting of the above parameters, the calculation formula for the establishment and micro increment matrix is as follows:

$$\Delta k_1(i,\, j) = \left| \frac{K_{ij} + K_{aj}}{2} - K_{aj} \right| \tag{8}$$

Substitute the results obtained from formula (8) into formula (9) to calculate the similarity between the composition and the micro increment:

$$\tau(i,\, j) = e^{\frac{1}{\Delta k_1(i,j)}} \tag{9}$$

On this basis, calculate the incremental product of energy demand, as follows:

$$\Delta k_2(i,\, j) = \left| \sqrt{K_{ij} K_{aj}} - K_{aj} \right| \tag{10}$$

Substitute the calculation result of formula (10) into formula (11) to calculate the product incremental similarity of the comprehensive energy demand. The process is as follows:

$$\sigma(i,\, j) = e^{\frac{1}{\Delta k_2(i,\, j)}} \tag{11}$$

Based on the above results, the distance similarity calculation formula for energy demand is:

$$SIM_1 = \beta \tau(i,\, j) + (1-\beta)\sigma(i,\, j) \tag{12}$$

In formula (12), β represents the distance coefficient.

4.1.2 Calculation of trend similarity in energy demand

Using segmented trend similarity synthesis to characterise the similarity features between data, and transforming them into multiple sets of dispersed numerical values, a new concept of trend line segment difference is introduced to achieve analysis of trend similarity between data (Li et al., 2021). Generally speaking, the shape similarity between different line segments can be analysed by the direct angle between the line segment and the horizontal axis. As the sequence is at the same time interval, this angle has higher comparability. Through the analysis of this angle, it can be found that the value of this angle only depends on the difference in longitudinal coordinates between the line and the line, and the difference between the scale value and the longitudinal coordinates in the direction of the line is determined as the value in the direction of the line (Wu et al., 2021b).

The geometric meaning of trend line segment values is shown in Figure 2.

Figure 2 Trend segment value (see online version for colours)

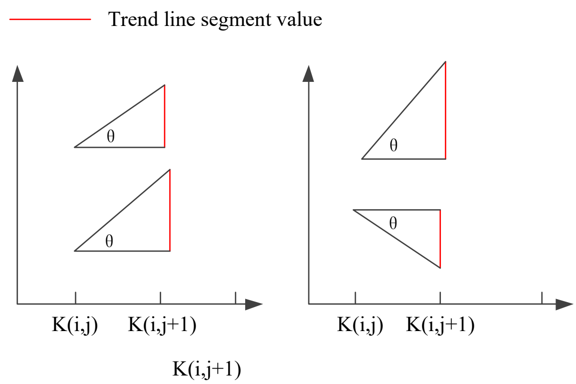

From Figure 2, it can be seen that there is a close relationship between the trend line segment values and the included angles, and they correspond one-to-one, reflecting the trend attributes of the line segment composed of adjacent two points. Whether it is a forward or reverse analogy, the trend curve values of each indicator can be directly compared and calculated, and its universality is significantly enhanced (Wang et al., 2022a). The calculation method for trend line segment difference is as follows:

$$\Delta k_3(i,\, j) = \left| \left[K_{a,j+1} - K_{aj} \right] = \left[K_{i,j+1} - K_{ij} \right] \right| \tag{13}$$

By using the calculation results of formula (13), the trend similarity of energy demand can be obtained, as follows:

$$SIM_2 = e^{\frac{1}{\Delta k_3(i,j)}} \tag{14}$$

By iteratively merging the calculation results of formula (12) and formula (14), the comprehensive similarity SIM of energy demand corresponding to the predicted day can be obtained. The calculation process is as follows:

$$SIM = \gamma \frac{1}{q} \sum_{j=1}^{q} SIM_1 + \mu \frac{1}{q-1} \sum_{j=1}^{q} SIM_2 \tag{15}$$

In formula (15), γ and μ represent a set of correlation coefficients, and the sum of the two is 1.

4.2 Prediction of comprehensive energy demand in parks based on echo state networks

As a unique form of neural network, echo state network has a simple training method, fast convergence speed, and can effectively solve complex nonlinear problems. It is particularly suitable for analysing non-stationary time series data (Tian et al., 2020). Therefore, after the above analysis and selection of similar daily energy demand data, this study uses echo state networks to predict the comprehensive energy demand of the park.

The structure of the echo state network is shown in Figure 3.

Figure 3 Echo state network structure diagram (see online version for colours)

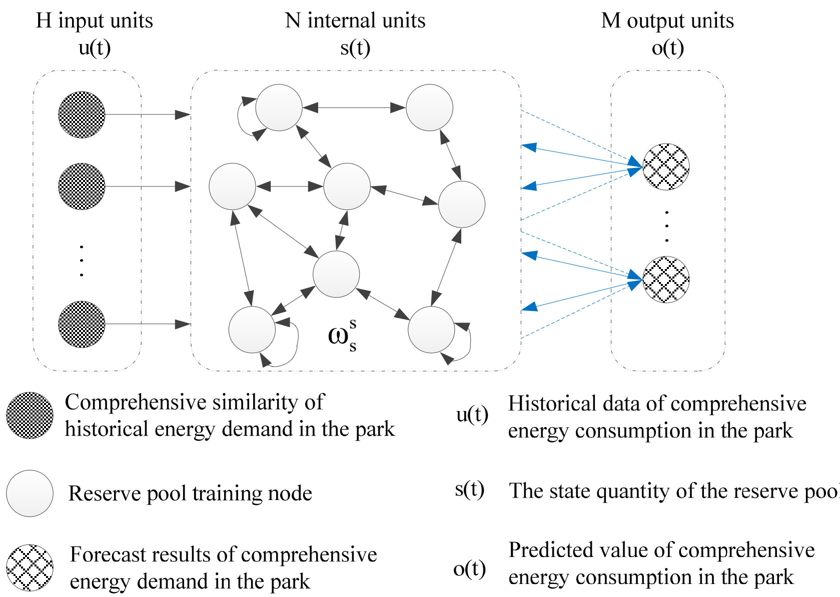

In the echo state network structure shown in Figure 3, the information of the input layer is the historical data of the comprehensive energy consumption of the park, and the output result of the output layer is the predicted value of the comprehensive energy consumption of the park.

In the echo state network, the input layer information at time t is defined as $u(t)$, the reserve pool state quantity is defined as $s(t)$, and the output layer information is defined as $o(t)$. The connection weights between the three parts are ω_u^s, ω_s^s and ω_s^o (Zhu et al., 2021).

The update formulas for the internal state $s(t)$ and output $o(t)$ of the reserve pool of the echo state network at time t are shown in formulas (16) and (17), respectively:

$$s(t) = f\left(\omega_u^s \times u(t) + \omega_s^s \times s(t-1) + \omega_s^o \times o(t-1)\right) \tag{16}$$

$$o(t) = f_{out}\left(\omega_s^o \times o(t-1)\right) \tag{17}$$

In the formula, $f(\cdot)$ represents the activation function in the reserve pool structure; $f_{out}(\cdot)$ represents the activation function of the output layer.

On this basis, in order to improve the performance of the echo state network, the crossbar algorithm is used to improve the connection weights of the echo state network. The process is as follows:

Process 1 Initialise the network according to the conditions.

Process 2 Perform horizontal crossover calculations and compare competition operators.

Process 3 Perform vertical crossover calculations and compare competition operators.

Process 4 Stop iteration.

Based on the analysis of the echo state network, the energy demand similar daily data obtained in Section 4.2 is input into the echo state network to predict the comprehensive energy demand of the park in the future stage. The specific steps are as follows:

Step 1 Collect historical consumption data of cooling/heating/electricity/gas loads in the comprehensive energy system of the park, and use interpolation and normalisation methods to preprocess the historical energy demand data according to the processes shown in formulas (3) and (4).

Step 2 Roughly select 12 dimensional influencing factors, calculate the mutual information value between influencing factors according to formula (6), and screen the influencing factors with the highest correlation according to the calculation results.

Step 3 According to the process of formulas (7)–(12), calculate the distance similarity SIM_1 of historical energy demand data.

Step 4 According to the process of formulas (13)–(14), calculate the trend similarity SIM_2 of historical energy demand data.

Step 5 Based on the results obtained from steps 3 and 4, calculate the total similarity SIM of historical energy demand data using formula (15).

Step 6 Construct a comprehensive energy demand load forecasting model using the echo state network, and improve the connection weights of the deep belief network using the cross over algorithm.

Step 7 Calculate load balance constraints. Different types of energy are converted through hub coupling devices to balance the energy demand at the load end. The conversion process between energy sources must be based on the law of conservation of energy, namely:

$$\Delta R_c = -\frac{w_c \eta_c}{w_d \eta_d} \Delta R_d \tag{18}$$

In formula (18), ΔR represents the change in energy consumption load; c and d represent the type of energy; W represents the unit calorific value of energy; η represents the utilisation rate of energy. Assuming that the total energy load that can meet the normal operation of the park is L_c, to ensure energy conservation, load balance constraints are introduced as follows:

$$L_c = -L_c^0 + \Delta L_c \left(s.t. \sum_{c=1}^{C} \Delta L_c = 0 \right) \tag{19}$$

In formula (19), L_c^0 represents the load before response; ΔL_c represents the energy load variation that can meet the normal operation of the park; C represents the type of energy.

Step 8 Use data from similar days of historical energy demand as input information for the echo state network, and after training in the reserve pool, output the predicted comprehensive energy demand of the park as follows:

$$Z = \frac{SIM}{L_c} \times o(t) \tag{20}$$

5 Experiment and result analysis

To verify the feasibility of the comprehensive energy demand prediction method for the park based on the echo state network designed above, the following experiments are designed.

5.1 Description of experimental environment

The experiment takes the cooling and heating load data of a certain park equipment company as an example and conducts simulation analysis in the MATLAB environment. The main energy supply methods of the comprehensive energy system in the park are combined cooling, heat and power generation, and photovoltaic power generation. The structure of the comprehensive energy system in the park is shown in Figure 4.

Figure 4 The comprehensive energy structure of the experimental park

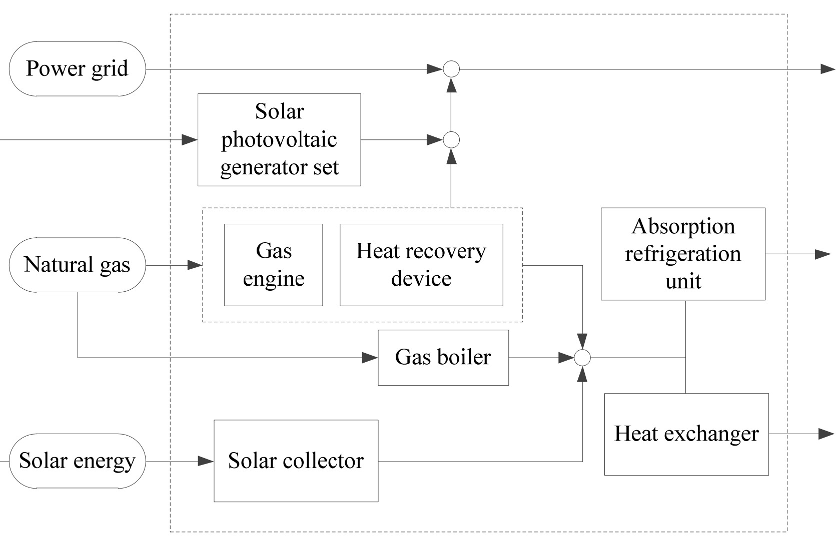

The simulation parameters of the park's energy supply indicators are shown in Table 1.

Table 1 Energy supply indicators

Project	*Numerical value*
Installed capacity	80 MW
Power generation output	65 MW
Annual heating capacity	839,041.7 Gj/a
Annual energy output	356.482 million kW/a
Annual power supply	37,418.3 million kW/a
Comprehensive auxiliary power consumption rate	3.0%
Annual average thermoelectric ratio	66%
Average annual power generation efficiency	45.63%
Average annual heating efficiency	73.15%

The basis for designing reasonable sample data for learning and validation is that the sample data should represent the characteristics of real data. Therefore, collect comprehensive energy consumption data of the park from January 2023 to April 2023 as samples, with a collection period of 0.5 hours. Collect data 48 times a day, and a total of 1,574 sample points were collected. During the experimental process, this study normalised the sample data and set the average length of the sample data to 8 Bytes. Randomly select half of the data as the training set and the other half as the testing set to predict the comprehensive energy demand of the park in the future stage. To avoid excessively single experimental results, the method of Wu et al. (2021a) and method of Xu et al.(2020) were compared and used together with the method of this paper to complete performance verification.

5.2 *Indicator description and result analysis*

In order to quantify the performance of various prediction methods, appropriate evaluation indicators were selected in the experiment to evaluate the prediction results of different prediction methods. The average absolute percentage error and standard error were selected as performance verification indicators in the experiment, and their calculation formulas are as follows:

$$MAPE = \frac{1}{n}\sum_{t=1}^{n}\frac{\overline{Y}_t - Y_t}{Y_t} \tag{21}$$

$$RMSE = \sqrt{\frac{1}{n}\sum_{t=1}^{n}\left(\overline{Y}_t - Y_t\right)^2} \tag{22}$$

In the formula, MAPE and RMSE represent the average absolute percentage error and standard error of the prediction results, respectively. n represents the number of sample points, $\overline{Y}_t$ represents the predicted comprehensive energy demand at time t, and Y_t represents the actual comprehensive energy demand corresponding to time t. Based on the above indicators, conduct performance analysis on different prediction methods.

Calculate the error situation of the comprehensive energy demand prediction for seven consecutive times, and the results are shown in Table 2.

Table 2 Error comparison of different prediction methods

Number of result statistics	*Method of this paper*		*Method of Wu et al. (2020)*		*Method of Xu et al. (2020)*	
	MAPE/%	*RMSE/MW*	*MAPE/%*	*RMSE/MW*	*MAPE/%*	*RMSE/MW*
1	2.051	178.7	5.553	345.5	5.283	363.7
2	2.112	198.3	6.586	275.5	4.677	496.9
3	2.362	184.7	6.358	361.4	4.595	555.0
4	1.410	205.3	7.582	494.0	5.974	452.5
5	2.250	176.4	6.564	339.9	4.849	404.6
6	1.967	195.4	5.854	546.6	4.363	579.2
7	2.384	203.0	6.353	453.6	5.431	433.3

Observing the data in Table 2, it can be seen that after applying the method of this paper, the MAPE value of the predicted results fluctuates between 1.410%–2.384%, and the RMSE value fluctuates between 176.4 MW–205.3 MW. On the other hand, the minimum MAPE value of method of Wu et al. (2020) is 5.553%, while the minimum MAPE value of method of Xu et al. (2020) is 4.363%. The minimum values of both predicted outcome indicators exceed the maximum value of method of this paper. The minimum RMSE index for method of Wu et al. (3030) is 275.5 MW, while the minimum RMSE index for method of Xu et al. (2020) is 363.7 MW, which still significantly exceeds the method of this paper.

Based on the above analysis, it can be concluded that the average absolute percentage error and root mean square error of the predicted results obtained by method of this paper are both low, indicating that the predicted results of method of this paper for the comprehensive energy demand of the park are closer to the actual comprehensive energy demand. The reason for the above results is that the method of this paper uses Lagrange polynomial to fill in the gaps in the historical data of comprehensive energy consumption in the park, effectively avoiding the impact of abnormal or missing data on the reliability of subsequent prediction. In addition, on the basis of initialising the echo state network, the method of this paper optimises key parameters such as echo state network weights and thresholds by crossing horizontally/vertically and comparing competition operators, thereby improving the prediction quality of the echo state network for the comprehensive energy demand of the park.

6 Conclusions

To accurately predict the demand for comprehensive energy in the park, this study collects and preprocesses historical comprehensive energy consumption data based on the analysis of the park's comprehensive energy structure. After data processing, it was found that the demand for comprehensive energy in the park is reflected in the demand for cooling/heating/electricity/gas loads. Therefore, four kinds of factors, temperature and humidity, wind speed and light, are selected as the influencing factors of energy demand prediction, and their average values and upper and lower limits are taken as the influencing factors. According to the analysis results of mutual information of the influencing factors, the distance similarity and trend similarity of historical energy demand are calculated. Through the iterative summation of the two factors, the comprehensive similarity of similar days of historical energy demand is calculated. Finally, the vertical and horizontal crossover algorithm is introduced to optimise the echo state network through horizontal/vertical crossover and comparison of competition operators. The comprehensive similarity is then input into the echo state network to obtain the final prediction result of the comprehensive energy demand of the park.

According to the experimental results, after applying the method of this paper:

1 The predicted MAPE value fluctuates between 1.410%–2.384%.

2 The RMSE value fluctuates between 176.4 MW–205.3 MW.

This can indicate that compared with the two traditional methods, the error of the method of this paper prediction results is significantly smaller, indicating that the method of this paper effectively achieves the design expectations.

Acknowledgements

This work was supported by State Grid Jiangsu Electric Power Design Consulting Co., Ltd., 'Research on Optimization of Site Selection, Configuration, and Design Scheme for Integrated Energy Station under Carbon Peaking and Carbon Neutrality Goals' (JE202103).

References

Fang, H., Ji, H. and Tian, S. (2020) 'Energy demand forecasting based on grey linear regression-fuzzy weighted Markov chain model', *Chinese Journal of Electron Devices*, Vol. 43, No. 5, pp.997–1003.

Huang, Z., He, G., Yan, H. and Tang, Y. (2020) 'Overview and prospect of optimization model function for community-scale integrated energy system', *Electric Power Automation Equipment*, Vol. 40, No. 1, pp.10–18.

Huang, Z., Xie, X. and Zhang, T. (2022) 'Medium-and long-term energy demand of china and energy transition pathway toward carbon neutrality', *Strategic Study of CAE*, Vol. 24, No. 6, pp.8–18.

Li, Z., Zhao, P., Wang, N. and Zhou, X. (2021) 'Multi-agent operation optimization of district integrated energy system based on reinforcement learning', *Proceedings of the CSU-EPSA*, Vol. 33, No. 12, pp.60–68.

Luo, J., Wen, Z., Dong, W., Li, Z., Liu, Z. and Wu, H. (2020) 'Model of integrated demand response potential based on portrait of residential users', *Renewable Energy Resources*, Vol. 38, No. 10, pp.1407–1414.

Tian, W., Yu, H., Li, P., Ji, H. and Wang, C. (2020) 'Projective integration-based dynamic simulation method for community integrated energy system with gas-electricity coupling', *Electric Power Automation Equipment*, Vol. 40, No. 11, pp.40–50.

Wang, L., Su, Z., Qiao, J. and Zhao, J. (2022a) 'Design of incremental regularized echo state network', *Control and Decision*, Vol. 37, No. 3, pp.661–668.

Wang, L., Wang, Y. and An, Z. (2022b) 'Echo state networks with improved particle swarm optimization algorithm for electricity demand forecasting', *Computer Engineering & Science*, Vol. 44, No. 8, pp.1457–1466.

Wu, W., Wu, J., Lei, Z., Zheng, M., Zhang, Y., Li, M., Huang, X. and Li, Y. (2021a) 'Park energy demand forecasting based on cso optimized deep belief network', *Power System Technology*, Vol. 45, No. 10, pp.3859–3868.

Wu, Z., Qi, S., Shang, M. and Shen, D. (2021b) 'Equivalent modeling of micro-grid using optimized ESN', *Acta Metrologica Sinica*, Vol. 42, No. 7, pp.923–929.

Xu, R., Wang, X., Zhao, Q. and Wang, S. (2020) 'A multi-energy demand prediction method based on convolutional neural network and deep belief network', *Distribution & Utilization*, Vol. 37, No. 10, pp.65–70.

Xue, M., Mao, X., Xiao, H., Pu, X. and Pei, W. (2022) 'A novel energy management method based on modified deep Q network algorithm for multi-park integrated energy system', *Electric Power Construction*, Vol. 43, No. 12, pp.83–93.

Zhang, F., Wu, D., Chen, Y., Feng, W., Zhang, Y. and Zhang, X. (2022) 'Economic scheduling strategy for integrated energy system in distributed parks based on multi-agent deep reinforcement learning', *Proceedings of the CSU-EPSA*, Vol. 34, No. 12, pp.18–26.

Zhang, N., Wang, H., Song, K., Cheng, M., Zhang, M. and Ye, P. (2023) 'Study on dynamic optimal control of integrated energy system based on multi-energy demand response', *Electrical Measurement & Instrumentation*, Vol. 60, No. 2, pp.16–24.

Zhao, H., Miao, S., Li, C., Zhang, D. and Tu, Q. (2022) 'Research on optimal operation strategy for park-level integrated energy system considering cold-heat-electric demand coupling response characteristics', *Proceedings of the CSEE*, Vol. 42, No. 2, pp.573–589.

Zheng, H., Zou, L., Yang, B., Xue, M., Tang, Y. and Wang, C. (2021) 'Three-level collaborative optimal design method of park-type integrated energy system with energy storage devices', *Science Technology and Engineering*, Vol. 21, No. 7, pp.2705–2712.

Zheng, Y., Zhang, A., Zhang, Y., Zhang, C. and Gou, L. (2022) 'Energy efficiency model of park-level integrated energy system considering time variation of equipment', *Smart Power*, Vol. 50, No. 4, pp.103–109.

Zhu, J., Dong, H., Li, S., Chen, Z. and Luo, T. (2021) 'Review of data-driven load forecasting for integrated energy system', *Proceedings of the CSEE*, Vol. 41, No. 23, pp.7905–7924.

Zhu, Z., Xu, Y., Cen, H., Huang, W., Zheng, J. and Li, Z. (2022) 'Optimal configuration of park-level integrated energy system considering demand response', *Smart Power*, Vol. 50, No. 1, pp.37–44.

Zhuo, Y., Chen, J., Zhu, J., Ye, H. and Wang, Z. (2022) 'Optimal scheduling of park-level integrated energy systems based on improved approximate dynamic programming', *High Voltage Engineering*, Vol. 48, No. 7, pp.2597–2606.